SiamIris: An Open Source Siamese Network for Iris Recognition

Daniel P. Benalcazar
DIMEC
Universidad de Chile
Santiago, Chile
dbenalcazar@ug.uchile.cl

Daniel Schulz
DIE
Universidad de Chile
Santiago, Chile
dschulz@ing.uchile.cl

Juan E. Tapia
Hochschule Darmstadt
da/sec-Biometrics and Internet Security Research Group
Darmstadt, Germany
juan.tapia-farias@h-da.de

***Abstract*—Iris recognition is one of the most reliable biometric systems on the market by virtue of the highly discriminative pattern of the human iris. The technique in which information is extracted from such pattern is crucial for good performance. Traditional methods are based on hand crafted filters for feature extraction, such as Gabor filters; on the other hand, state of the art methods rely on features extracted from convolutional networks pre-trained on ImageNet. In this work, we propose to use the Siamese Network architecture to optimize the extracted features for Iris recognition. This is achieved by training the network to assert whether two iris images belong to the same subject or not. The proposed architecture, SiamIris, was trained on Notre Dame´s dataset and tested against state-of-the-art systems, producing reasonable performance for the small number of training subjects used.**

I. Introduction

The human iris has a very distinctive texture that is ideal for verification and identification, especially in the Near Infrared (NIR) spectrum [1]. John Daugman proposed to represent this complex texture in a compact iris code that is easy to compare from subject to subject [2]. Over time, iris recognition methods have improved using both image processing and deep learning techniques. Nowadays, Iris Recognition is one of the most reliable biometric modalities [3].

The process of iris recognition consists of image acquisition, segmentation, localization, normalization, feature extraction and comparison [2], [3]. The feature extractor in traditional iris recognition systems is based on hand-crafted filters, such as Gabor wavelets [2], Localized Binary Patterns (LBP) [4], Binarized Statistical Image Features (BSIF) [5], [6], and 3D descriptors [7], [8]. They produce strong features that help in the identification task. However, a question rises on whether they are the best possible filters that could be obtained or not [9].

On the other hand, more modern iris recognition systems [10], [10]–[13] rely on features extracted using convolutional neural networks (CNN) pre-trained on ImageNet [14]. Those features are also strong since the network had observed numerous complex patterns in the input images that help classify them in a thousand different classes [15]. That is why, the strong features produced by pre-trained networks can be successful for different tasks, like iris recognition, even without fine tuning [13]. The problem with this approach is that ImageNet CNNs have been trained to produce similar features for objects of the same class: eyes. There is no emphasis in producing distinctive features for each iris. Choosing earlier layers [11], [13], as well as a fine-tunning process can certainly increase the performance of the network [16]. Another problematic is the scarcity of Iris Recognition models openly available of researches to improve or compare against.

That is why we propose SiamIris (Figure 1), an open source network that uses the siamese architecture [17] to train CNNs for the specific purpose of Iris Recognition. For the network's input, the use of two types of images is compared: periocular iris images (Figure 1a) and normalized iris images (Figure 1b), also known as Rubber Sheet [2]. Then, the network must determine if two irises being compared are mated or non-mated according to the euclidean distance between the network's embeddings. Using periocular images presents the additional advantage of skiping the segmentation step; thus, reducing the computational cost of the segmentation and localization steps needed in traditional Iris Recognition.

In this scope, the contributions of this work are as follows.

- Open Source Model: The Siamese Network architecture is used for the purpose of Iris Recognition. Our best trained models will be made freely available.
- Training Process: Training scheme involving hard triplet loss is thoughtfully explained.
- Evaluation: This method is evaluated on the Notre Dame LG4000 dataset [18], and the performance is compared with state-of-the-art methods.

In the following sections, we expand on the related methods in Section II, the dataset used is explained in Section III, SiamIris' architecture and the training process are explained in Section IV, the important Metrics used for evaluation are defined in Section V, the results are illustrated in Section VI, finally concluding in Section VII.

II. Related Work

The human iris has a very distinctive texture that is ideal for verification and identification, especially in the Near Infrared

This work is supported by the German Federal Ministry of Education and Research and the Hessian Ministry of Higher Education, Research, Science and the Arts within their joint support of the National Research Center for Applied Cybersecurity ATHENE.

978-1-6654-8744-3/22/$31.00 ©2022 IEEE

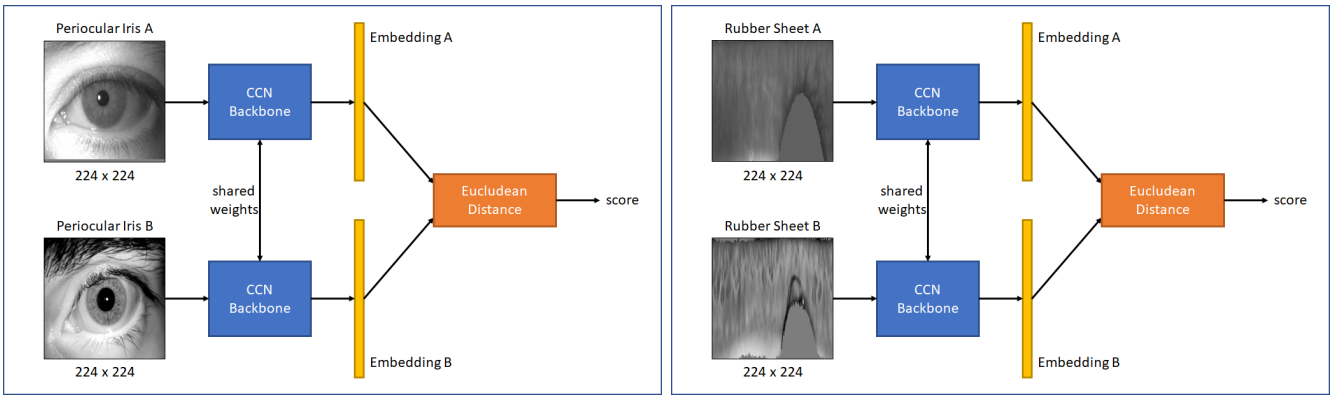

Fig. 1. SiamIris Architecture. This Siamese network predicts whether two irises come from to the same subject or different subjects. a) Using periocular iris images as inputs. b) Using Rubber Sheet images as inputs.

(NIR) spectrum [1]. John Daugman proposed to represent this complex texture in a compact iris code that is easy to compare from subject to subject [2]. This iris code is the result of applying Gabor wavelets over a normalized iris image, in polar coordinates, and capturing the phase-quadrant information only [2]. Popular frameworks have implemented this approach, such as IREX [19], [20] and Osiris [21]. Zhaofeng et al. proposed to use LBP as an alternative to Gabor wavelets [4]. BSIF filters have also been used in iris recognition with good performance [6], [9]. In recent years, the 3D relief of the iris surface has also been captured and encoded for iris recognition [7], [7]. Finally, deep learning methods have produced great results in iris recognition [13], [22].

After the great success of deep learning for image classification, this technique was quickly adapted in iris recognition [22]. Gangwar and Yoshi developed DeepIrisNet, a CNN that encodes the iris texture in a robust manner with good accuracy even under cross-sensor identification [10]. Zhao and Kumar proposed UniNet, a two-path network that generates the encoding of the iris texture as well as a binary mask that predicts the probability of each element in the feature vector of coming from iris and non-iris regions [12]. Nguyen et al. tested the iris recognition performance of several pretrained CNNs [11]. Since those networks have developed strong feature extractors for image classification on ImageNet [14], it was natural to assume that they would be suitable for encoding the iris texture. Nguyen et. al [11], as well as Zambrano et. al [13] explored the best layer of each network to extract features from, achieving state-of-the-art performance. Zambrano even proposed a novel masking technique to avoid the influence of eye-leads and eyelashes in intermediate layers of the network. Wang and Kumar considered residual networks with dilated convolutional kernels to optimize the training process [23]. Zhao et al. implemented a method based on capsule network architecture with great performance [23]. Minaee et al. [24] developed DeepIris based on residual layers and used the entire iris image instead of the rubber sheet. Adamovic et al. combined stylometric feature extraction with machine learning techniques to produce a novel approach [24]. Additionally, images produced by generative adversarial networks have been used to enhance the training dataset [25], [26].

The works of Czajka et al. [9] and Boyd et al. [16] started challenging weather off the shelf BSIF and CNN feature extractors were the best choice for iris recognition. Czajka et al. performed domain adaptation over standard BSIF filters to learn human-inspired features useful for iris recognition [9]. Their best model outperformed non-trained BSIF filters and standard methods like Osiris [9], [21]. Boyd et al. compared the performance of iris-specific trained ResNet-50 models against that of ResNet-50 trained for non-iris tasks [16]. They discovered that fine tuning a model for iris recognition obtained greater accuracy than off-the-shelf models and training from scratch [16]. Their best model also produced state-of-the-art results [16].

Additionally, siamese networks [17] have been trained to obtain specific filters for biometric tests since the one-shot-learning paradigm is very similar to the identity verification task. Zhang et al. developed two siamese network architectures for face recognition, which were trained from scratch using face images [27]. Song et al. also developed a face recognition method with state-of-the-arts results [28]. Zhong et al. implemented a palmprint recognition method using a siamese network with VGG-16 as the backbone [29]. They only fine-tuned the final two fully connected layers with palmprint images to obtain good results with a small image set [29]. Ridha and Saud started using siamese networks for iris recognition [30]. They also implemented a learnable mutual-component distance that allowed their method to obtain good performance even under heterogeneous device conditions [30]. Parzianello and Czajka developed a contact-lens-aware iris-recognition method using siamese networks [31].

III. Dataset

In this work we use the Notre Dame Dataset [18] captured with the Near-Infrarred-Range (NIR) LG-4000 sensor, as described in [32]. The authors separated as different identities

(IDs) the left and right eyes of each subject; thus, the dataset was named ND-LG400-LR [32]. There are 811 IDs and 10,959 images in total, comprised of 5,476 left-eye and 5,483 right-eye images. Table I indicates the number of IDs images and comparisons in the train, test and validation splits. The splits were constructed in a person-disjoint manner. As Table I indicates, the dataset has only 487 IDs for training, which is very challenging.

In Section VI we contrast the performance of SiamIris against state-of-the-art methods [9], [13] that require rubber sheets. Since the main focus of this work is contrasting the feature extraction capabilities of each method, we standardize the segmentation stage by using the same rubber sheet images for all the methods tested. First, a periocular iris image (Figure 2a) is segmented using the DenseNet10 network [33]. The result is a semantic segmentation mask of the valid pixels of the iris (Figure 2b). Then, the circles that best bit pupil an iris are found using the LMS algorithm [33]. Finally the iris is unwrapped using polar coordinates, as illustrated in Figure 2d. We used the open source method of Fang et. al [34] for this step. The result is the normalized iris image, also known as rubber sheet (Figure 2e). All the rubber sheeets in Table I were created with this pipeline.

TABLE I
DESCRIPTION OF THE ND-LG4000-LR DATASET

Description	Test	Train	Val
Identities (IDs)	162	487	162
Periocular Images	2,090	6,663	2,203
Rubber Sheets	2,090	6,663	2,203
Mated Comparisons	19,029	66,114	22,109
Non-mated Comp.	105,470	1,079,445	117,367

IV. METHODOLOGY

Our method consists of a siamese network as illustrated in Figure 1. It takes two periocular iris images as the input and it outputs the similarity in base of the Eucliedean distance between the embeddings produced by the CNN. In Figure 1 this is depicted as the two images passing through two identical copies of the CNN block, but in practice, only one copy is stored in memory and it takes the two images, producing the two embeddings. For the CNN backbone block, both Resnet50 [35] and MobileNetV2 [36] were used separately, and in Section VI their performances are compared. Additionally, we compare the use of periocular iris images (Figure 2a) against using rubber sheet images (Figure 2e). For both backbones, the input images are sesized to 224×224 before being processed by the network. The size of the embeddings is $1 \times 2,048$ for ResNet50 and $1 \times 1,792$ for MobileNetV2.

Both backbone networks were fine-tuned from the available ImageNet [14] weights. For the Resnet50 backbone, the following hyperparamenters were used: unfreazing from layer "conv5_block2_out", batch size of 1024, learning rate of 10-5, 400 epochs and Adam optimization. For the MobileNetV2 backbone, the best results were obtained using the following

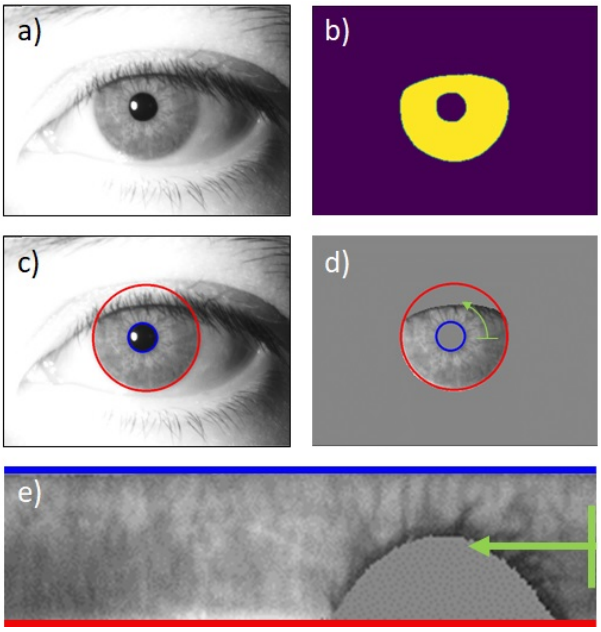

Fig. 2. Image pre-processing steps. a) Input image. b) Iris mask predicted by CCNet. c) Iris and pupil localization using the mixed algorithm. d) Isolated iris. e) Rubber-sheet model. Blue lines represent the pupil-iris boundary, while red lines represent the iris-sclera boundary. The green arrows in d) and e) represent the direction in which the iris was unwrapped.

hyperparameters: altpha parameter multiplication of 1.4, unfreezing from layer "block_16_expand", batch size of 512, learning rate of 10-5, 300 epochs and Adam optimization. The best performing SiamIris model will be made publicly available on GitHub[1] (upon acceptance).

During training, all the networks used the Hard Triplet Loss [37] function. For the computation of the Triplet Loss, tree images are involved: an anchor image, an image with the same ID as the anchor, and one image with a different ID. In this way, the network learns to minimize the distance between images of the same ID while maximizing the distance of images of different IDs. Triplets are formed within the batch for better training efficiency.

V. METRICS

The d-prime (d') metric assesses the separation between the mated and non-mated distributions. The higher the value is better. It is computed using (1) [2], where μ_m and μ_n are the mean of the mated and non-mated distributions respectively, and σ_m and σ_n are the standard deviations.

$$d' = \frac{|\mu_m - \mu_n|}{\sqrt{0.5 \times (\sigma_m^2 + \sigma_n^2)}} \tag{1}$$

The False Match Rate (FMR) is the number of comparisons falsely classified as mated divided by the number of non-mated comparisons. Likewise, the False Non-Match Rate (FNMR) is the number of comparisons falsely classified as non-mated divided by the number of mated comparisons. Both metrics

[1]https://github.com/dpbenalcazar/SiamIris-v1

TABLE II
RESULTS ON THE ND-LG4000-LR DATASET

Method	d'	EER [%]	$FNMR_{10}$ [%]	$FNMR_{20}$ [%]	$FNMR_{100}$ [%]
ICA Filters [9]	5.822	0.5203	0.2155	0.2943	0.4204
DenseNet201 [13]	3.178	0.9842	0.3206	0.5308	0.9669
SiamIris R50-iris (ours)	4.457	1.5720	0.2680	0.5097	2.4752
SiamIris R50-rubb (ours)	4.137	2.3865	0.5045	1.1193	4.8872
SiamIris MN2-iris (ours)	3.898	2.5960	0.4256	1.0983	5.2551
SiamIris MN2-rubb (ours)	3.855	2.9449	0.6779	1.6396	7.9826

in tandem give the performance of the system for a given operation point.

In this work, four operation points are considered: Equal Error Rate (EER), $FNMR_{10}$, $FNMR_{20}$ and $FNMR_{100}$. The EER is the point in which FMR equals FNMR. On the other hand, $FNMR_{10}$, $FNMR_{20}$ and $FNMR_{100}$ are the points in which FMR is at 10%, 5% and 1% respectively. All those operating poins can be seen in the Detection Error Trade-off (DET) curve.

VI. RESULTS

Four configurations of SiamIris were evaluated, changing the backbones and type of input images. ResNet50 with iris images (SiamIris R50-iris), ResNet50 with rubber sheets (R50-rubb), MobileNetV2 with iris images (SiamIris MN2-iris), and MobileNetV2 with with rubber sheets (MN2-rubb). The four models were trained with the train and validation partitions indicated in Table I and using the hyperparameters explained in Section IV.

We compared the performance of the 4 SiamIris models against state-of-the-art methods such as Czajka's ICA filters [9], [34] and Zambrano's best network, based on DenseNet201 [13], [38]. All evaluations were conducted in the test set of the ND-LG400-LR dataset described in Table I.

Figure 3 shows the DET curves of all the 6 methods compared, along with their EER values. It can be seen that the ICA filters [9], [34] obtained the best overall results, followed by Zambrano's method [13]. These methods obtained EER values of 0.52% and 0.98% respectively. Among the four SiamIris variations, the one using ResNet50 and iris images obtain the best performance, with EER=1.57%. This method is just 1% below the performance of the best overall method. Finally, the remaining 3 variarions of SiamIris obtaines EER values between 2% and 3%.

Table II reports the metrics of the 6 methods in more detail. For the d' score, higher is better, but for the rest lower is better. The overall trends observed in Figure 3 can be seen in Table II as well. However, looking at the d' value, all SiamIris networks presented better performance than Zambrano's method [13]. Something similar happends at the $FNMR_{10}$ operating point, where SiamIris R50-iris has an smaller error than Zambrano's method [13], and its performances is just 0.05% below the ICA filters [9], [34].

VII. CONCLUSIONS

We proposed SiamIris, an open source siamese network trained for Iris Recognition. The best configuration resulted

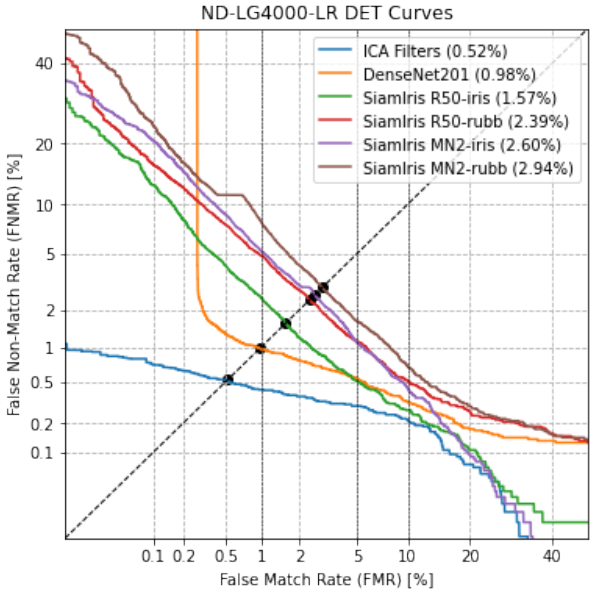

Fig. 3. DET curves of the evaluated methods on the ND-LG4000-LR dataset. The EER of each method is indicated in parenthesis.

using a ResNet50 backbone with periocular iris images as the input, which does not requiere a segmentation stage. That configuration produced close to state-of-the-art performance since the EER and $FNMR_{10}$ were just 1% and 0.05% worse than the best performing method (ICA filters [9], [34]). Those levels of performance were obtained despite the fact that only 487 IDs were used for training. We hypothesize that performance could be increased in datasets with higher number of subjects.

Future work includes developing a custom backbone, training and evaluating on bigger datasets, and using synthetic iris images [39], [40] to increase the available subjects.

ACKNOWLEDGMENT

This work is supported by the German Federal Ministry of Education and Research and the Hessian Ministry of Higher Education, Research, Science and the Arts within their joint support of the National Research Center for Applied Cybersecurity ATHENE.

REFERENCES

[1] K. W. Bowyer, K. Hollingsworth, and P. J. Flynn, "Image understanding for iris biometrics: A survey," *Computer vision and image understanding*, vol. 110, no. 2, pp. 281–307, 2008.

[2] J. Daugman, "How iris recognition works," in *The essential guide to image processing*. Elsevier, 2009, pp. 715–739.

[3] K. W. Bowyer and M. J. Burge, *Handbook of iris recognition*. Springer, 2016.

[4] Z. He, Z. Sun, T. Tan, and Z. Wei, "Efficient iris spoof detection via boosted local binary patterns," in *International conference on biometrics*. Springer, 2009, pp. 1080–1090.

[5] K. B. Raja, R. Raghavendra, and C. Busch, "Binarized statistical features for improved iris and periocular recognition in visible spectrum," in *2nd International Workshop on Biometrics and Forensics*. IEEE, 2014, pp. 1–6.

[6] C. Rathgeb, F. Struck, and C. Busch, "Efficient bsif-based near-infrared iris recognition," in *2016 Sixth International Conference on Image Processing Theory, Tools and Applications (IPTA)*. IEEE, 2016, pp. 1–6.

[7] D. P. Benalcazar, J. E. Zambrano, D. Bastias, C. A. Perez, and K. W. Bowyer, "A 3d iris scanner from a single image using convolutional neural networks," *IEEE Access*, vol. 8, pp. 98 584–98 599, 2020.

[8] D. P. Benalcazar, D. A. Montecino, J. E. Zambrano, C. A. Perez, and K. W. Bowyer, "3d iris recognition using spin images," in *2020 IEEE International Joint Conference on Biometrics (IJCB)*. IEEE, 2020, pp. 1–8.

[9] A. Czajka, D. Moreira, K. Bowyer, and P. Flynn, "Domain-specific human-inspired binarized statistical image features for iris recognition," in *2019 IEEE Winter Conference on Applications of Computer Vision (WACV)*. IEEE, 2019, pp. 959–967.

[10] A. Gangwar and A. Joshi, "Deepirisnet: Deep iris representation with applications in iris recognition and cross-sensor iris recognition," in *2016 IEEE international conference on image processing (ICIP)*. IEEE, 2016, pp. 2301–2305.

[11] K. Nguyen, C. Fookes, A. Ross, and S. Sridharan, "Iris recognition with off-the-shelf cnn features: A deep learning perspective," *IEEE Access*, vol. 6, pp. 18 848–18 855, 2017.

[12] Z. Zhao and A. Kumar, "Towards more accurate iris recognition using deeply learned spatially corresponding features," in *Proceedings of the IEEE international conference on computer vision*, 2017, pp. 3809–3818.

[13] J. E. Zambrano, D. P. Benalcazar, C. A. Perez, and K. W. Bowyer, "Iris recognition using low-level cnn layers without training and single matching," *IEEE Access*, vol. 10, pp. 41 276–41 286, 2022.

[14] J. Deng, W. Dong, R. Socher, L.-J. Li, K. Li, and L. Fei-Fei, "Imagenet: A large-scale hierarchical image database," in *2009 IEEE conference on computer vision and pattern recognition*. Ieee, 2009, pp. 248–255.

[15] K. He, X. Zhang, S. Ren, and J. Sun, "Deep residual learning for image recognition," in *Proceedings of the IEEE conference on computer vision and pattern recognition*, 2016, pp. 770–778.

[16] A. Boyd, A. Czajka, and K. Bowyer, "Deep learning-based feature extraction in iris recognition: Use existing models, fine-tune or train from scratch?" in *2019 IEEE 10th International Conference on Biometrics Theory, Applications and Systems (BTAS)*. IEEE, 2019, pp. 1–9.

[17] G. Koch, R. Zemel, R. Salakhutdinov *et al.*, "Siamese neural networks for one-shot image recognition," in *ICML deep learning workshop*, vol. 2. Lille, 2015.

[18] U. of Notre Dame USA, "Crosssensor-iris-2012-data-set," 2012. [Online]. Available: https://cvrl.nd.edu/projects/data/#nd-crosssensor-iris-2012-data-set

[19] P. Grother, E. Tabassi, G. Quinn, and W. Salamon, "Irex i-performance of iris recognition algorithms on standard images-nist interagency report 7629," *National Institute of Standards and Technology. Information Access Division. http://www. nist. gov/itl/iad/ig/irexi. cfm*, 2009.

[20] G. W. Quinn, J. Matey, E. Tabassi, and P. Grother, "IREX V Guidance for Iris Image Collection NIST Interagency Report 8013 Information Access Division National Institute of Standards and Technology," 2014.

[21] N. Othman, B. Dorizzi, and S. Garcia-Salicetti, "Osiris: An open source iris recognition software," *Pattern Recognition Letters*, vol. 82, pp. 124–131, 2016.

[22] A. Boyd, S. Yadav, T. Swearingen, A. Kuehlkamp, M. Trokielewicz, E. Benjamin, P. Maciejewicz, D. Chute, A. Ross, P. Flynn *et al.*, "Post-mortem iris recognition—a survey and assessment of the state of the art," *IEEE Access*, vol. 8, pp. 136 570–136 593, 2020.

[23] K. Wang and A. Kumar, "Toward more accurate iris recognition using dilated residual features," *IEEE Transactions on Information Forensics and Security*, vol. 14, no. 12, pp. 3233–3245, 2019.

[24] S. Minaee and A. Abdolrashidi, "Deepiris: Iris recognition using a deep learning approach," *arXiv preprint arXiv:1907.09380*, 2019.

[25] S. Adamović, V. Miškovic, N. Maček, M. Milosavljević, M. Šarac, M. Saračević, and M. Gnjatović, "An efficient novel approach for iris recognition based on stylometric features and machine learning techniques," *Future Generation Computer Systems*, vol. 107, pp. 144–157, 2020.

[26] M. B. Lee, Y. H. Kim, and K. R. Park, "Conditional generative adversarial network-based data augmentation for enhancement of iris recognition accuracy," *IEEE Access*, vol. 7, pp. 122 134–122 152, 2019.

[27] X. Sun, G. Han, L. Guo, T. Xu, J. Li, and P. Liu, "Updatable siamese tracker with two-stage one-shot learning," *arXiv preprint arXiv:2104.15049*, 2021.

[28] J. Zhang, X. Jin, Y. Liu, A. K. Sangaiah, and J. Wang, "Small sample face recognition algorithm based on novel siamese network," *Journal of Information Processing Systems*, vol. 14, no. 6, pp. 1464–1479, 2018.

[29] L. Song, D. Gong, Z. Li, C. Liu, and W. Liu, "Occlusion robust face recognition based on mask learning with pairwise differential siamese network," in *Proceedings of the IEEE/CVF International Conference on Computer Vision*, 2019, pp. 773–782.

[30] D. Zhong, Y. Yang, and X. Du, "Palmprint recognition using siamese network," in *Chinese conference on biometric recognition*. Springer, 2018, pp. 48–55.

[31] J. A. Ridha and J. H. Saud, "Mutual component convolutional siamese network for heterogeneous iris recognition."

[32] D. P. Benalcazar, J. E. Tapia, M. Vasquez, L. Causa, E. L. Droguett, and C. Busch, "Towards an efficient iris recognition system on embedded devices," *arXiv preprint arXiv:2210.13101*, 2022.

[33] J. E. Tapia, E. L. Droguett, A. Valenzuela, D. P. Benalcazar, L. Causa, and C. Busch, "Semantic segmentation of periocular near-infra-red eye images under alcohol effects," *IEEE Access*, vol. 9, pp. 109 732–109 744, 2021.

[34] Z. Fang and A. Czajka, "Open source iris recognition hardware and software with presentation attack detection," in *2020 IEEE International Joint Conference on Biometrics (IJCB)*. IEEE, 2020, pp. 1–8.

[35] K. He, X. Zhang, S. Ren, and J. Sun, "Deep residual learning for image recognition," in *Proceedings of the IEEE conference on computer vision and pattern recognition*, 2016, pp. 770–778.

[36] A. G. Howard, M. Zhu, B. Chen, D. Kalenichenko, W. Wang, T. Weyand, M. Andreetto, and H. Adam, "Mobilenets: Efficient convolutional neural networks for mobile vision applications," *arXiv preprint arXiv:1704.04861*, 2017.

[37] F. Schroff, D. Kalenichenko, and J. Philbin, "Facenet: A unified embedding for face recognition and clustering," in *Proceedings of the IEEE conference on computer vision and pattern recognition*, 2015, pp. 815–823.

[38] G. Huang, Z. Liu, L. Van Der Maaten, and K. Q. Weinberger, "Densely connected convolutional networks," in *Proceedings of the IEEE conference on computer vision and pattern recognition*, 2017, pp. 4700–4708.

[39] J. Maureira, J. E. Tapia, C. Arellano, and C. Busch, "Analysis of the synthetic periocular iris images for robust presentation attacks detection algorithms," *IET Biometrics*, 2022.

[40] D. P. Benalcazar, D. A. Benalcazar, and A. Valenzuela, "Artificial pupil dilation for data augmentation in iris semantic segmentation," in *2022 IEEE Sixth Ecuador Technical Chapters Meeting (ETCM)*. IEEE, 2022, pp. 1–6.